International Journal of Latest Engineering and Management Research (IJLEMR)
ISSN: 2455-4847
www.ijlemr.com || REETA-2K16 ǁ PP. 80-89

A LEAD-LAG CONTROLLER WITH FUZZY ADVANCED CONTINUOUS ANT COLONY OPTIMIZATION USED IN CONTROL OF FLEXIBLE AC TRANSMISSION SYSTEM DEVICES

M.lokanadham[1], B.Devendar[2], A.Naveen kumar[3]
[1]*Assistant professor, SVPCET*
[2]*P.G STUDENT, SVPCET*
[3]*P.G STUDENT, SVPCET*

Abstract: This paper proposes an evolutionary fuzzy lead-lag control approach for coordinated control of flexible AC transmission system (FACTS) devices in a multi-machine power system. The FACTS devices used are a thyristor-controlled series capacitor (TCSC) and a static var compensator (SVC), both of which are equipped with a fuzzy lead-lag controller to improve power system dynamic stability. The fuzzy lead-lag controller uses a fuzzy controller (FC) to adaptively determine the parameters of two lead-lag controllers at each control step according to the deviations of generator rotor speeds. This paper proposes an Advanced Continuous Ant Colony Optimization (ACACO) algorithm to optimize all of the free parameters in the FC, which avoids the time-consuming task of parameter selection by human experts. The effectiveness and efficiency of the proposed evolutionary fuzzy lead-lag controller for oscillation damping control is verified through control of a multi-machine power system and comparisons with other lead-lag controllers and various population-based optimization algorithms.

Index Terms: Ant colony optimization, flexible AC transmission system (FACTS), fuzzy control, static var compensator (SVC), swarm intelligence, thyristor controlled series capacitor (TCSC).

I. INTRODUCTION

POWER SYSTEM (PS) stability control is an important task in PS operation . Several factors, such as external disturbances or internal mechanical torques, may easily affect system stability. With the development of power electronics, the structural control of electric power networks has recently attracted more attention. In this context, flexible AC transmission system (FACTS) devices are becoming more popular. Due to their fast response, these devices are used to dynamically adjust the network configuration to enhance steady-state performance as well as dynamic stability . The availability of FACTS devices, Such as thyristor-controlled series compensators (TCSCs), static var compensators (SVCs), and static synchronous series compensators (SSSCs), can provide variable turn and/or series compensation . However, these devices can interfere with one another. When the Controller parameters of a dynamic device are tuned to obtain the best performance, control conflicts that arise between various FACTS controllers may lead to the onset of oscillations . Thus, the coordinated control of these devices is very important . TCSCs and SVCs have been widely studied in the technical literature and have been shown to significantly enhance system stability . Therefore, this paper employs these two devices and proposes a new coordinated control scheme to enhance the dynamic response of a multi-machine PS. Different FACTS device control methods have been proposed for power oscillation damping and transient stability improvement . One popular damping control method uses a washout filter followed by the order lead-lag controller . In general, the parameters of a lead lag controller are designed using the pole-zero location method . Modern PSs are large-scale and complex. Disturbances typically change the network topology and result in a nonlinear response. Therefore, capabilities of traditional control laws based on liberalized models are limited. To address this problem, FACTS control using fuzzy control scheme has been proposed . Unlike previous control configurations, this paper proposes a fuzzy lead-lag control scheme for the control and coordination of TCSC and SVC devices in a multi-machine PS. In this new control configuration, an FC is designed to adaptively adjust the parameters of lead-lag controllers at each control time step. Performance advantage of the FACTS devices equipped with the fuzzy lead-lag controller is verified through comparison with traditional lead-lag controllers. Evolutionary fuzzy systems that design fuzzy systems population-based evolutionary computation techniques have drawn attention in the past two decades. In contrast to genetic algorithms and particle swarm optimization (PSO) , continuous ACO, which finds solutions in a continuous space, is a relatively new optimization approach . Instead of using existing continuous ACO algorithms, this paper proposes a novel ACO algorithm called Advanced Continuous Ant Colony Optimization (ACACO).

ACACO is used to optimize all of the free parameters in the FC to simplify the design effort and improve PS control performance.

The performance of ACACO is verified through comparisons with various PSO and ACO algorithms. This paper is organized as follows. Section II describes the FACTS model. Section III introduces the fuzzy lead-lag control configuration. Section IV introduces the proposed ACACO.

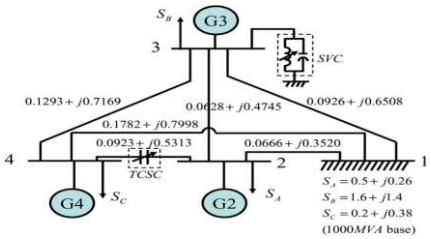

Fig.1. Multi-power system.

Section V describes four examples of FACTS control problems. The performance of the proposed evolutionary fuzzy lead-lag control configuration is compared with that of different evolutionary control approaches. Finally, Section VI presents the conclusion.

II. SYSTEM MODEL

Fig. 1 shows a single-line diagram of the studied system consisting of three machines, three static loads, and an interconnecting network including mutually-coupled transmission lines radially connected to an infinite bus . The excitation system for the synchronous generator is the IEEE type 1 excitation system with constant prime mover mechanical torque. The system data are given in the Appendices. The dynamic behaviors of the generators are described by the nonlinear one-axis model with a rotor reference frame. At a nominal operating point, the nonlinear dynamic equations are first literalized to obtain a set of linear state equations with which we can examine the small-signal stability of the system with Eigen value analysis. The electromechanical modes are close to the imaginary axis of the complex plane. The damping for the three dominant modes needs to be increased, and the requirement for appropriate stabilization equipment to damp out the multi-machine PS oscillations is evident. The TCSC is inserted into the transmission line between bus 2 and bus 4 to control the power flow. The SVC is placed at the generator bus 3 to provide instantaneous reactive power modulation for voltage maintenance. To create better continuous operating characteristics and a better application, a complete TCSC system is made up of several single-module TCSCs in series to fill in the gaps between operation modes, as shown in Fig. 2. The block diagram for the TCSC model for typical transient and oscillatory stability studies is shown in Fig. 3 . There are three inputs for various purposes: an auxiliary signal, , which could be the input from an external power flow controller, the reference, which is the initial operating point of the TCSC, and the small-signal modulation input, , to provide stability.

The configuration of a fixed capacitor thyristor-controlled reactor (TCR) SVC is shown in Fig. 4. The nonlinear equivalent block diagram of the TCR part of the SVC is shown in Fig. 5. The equivalent admittance of the TCR can be obtained from

$$B_L(\alpha) = \left[\frac{2\pi - 2\alpha + \sin 2\alpha}{\pi}\right] B_{L\,MAX} \qquad (1)$$

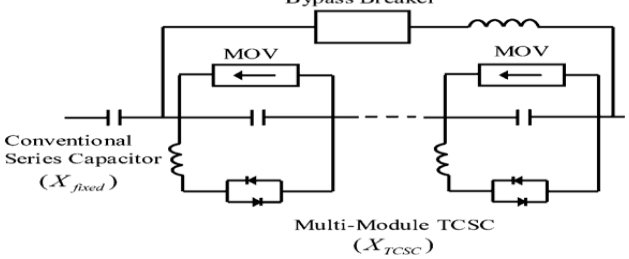

Fig. 2. Configuration of multimode TCSCs.

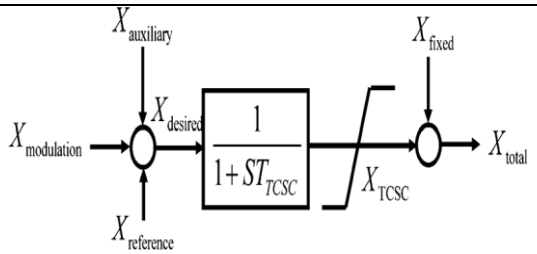

Fig. 3. Block diagram of TCSC model.

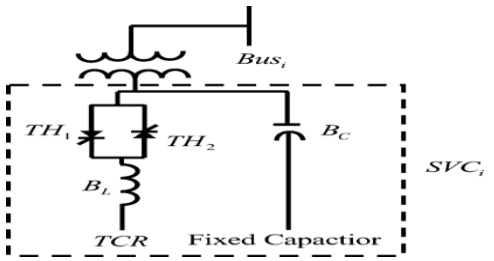

Fig. 4. Configuration of fixed capacitor-TCR SVCs.

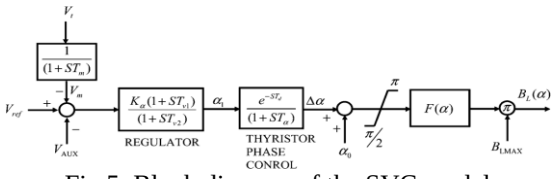

Fig.5. Block diagram of the SVC model

Where is the total admittance of the reactors relative to its MVA rating. The auxiliary controllers can give an additional control signal to the voltage regulator terminal. For an interconnected system with a large number of generating units, such as in the order of 1000, detailed modeling the system of each individual generator is far too complex to design a controller easily. Simpler models with lower dimension give much more understandable design procedure and results. The Three-machine PS studied is simple but the proposed method is quite general and hence the application to more complex cases can be easily implemented by PS dynamic model reduction [25].

III. EVOLUTIONARY FUZZY LEAD-LAG CONTROL CONFIGURATION

The selection of control inputs is very critical for wide area control. The most often used method to select locations and

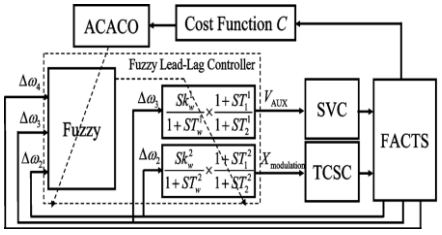

Fig. 6. Evolutionary fuzzy lead-lag control configuration.

stabilizing signals for PSSs and FACTS devices is controllability observability analysis based on a linearized time-invariant system model around a given operating condition . Since our proposed design method is applied directly to a nonlinear system model, conventional generator rotor speed deviations are selected as control inputs conservatively.

A. Lead-Lag Controller

This paper employs two lead-lag controllers to provide suitable control signals to the TCSC and the SVC.

$$\frac{V_{AUX}}{\Delta_{\omega 3}} = \frac{SK_{\omega}^{1}}{1+ST_{W}^{1}} X \frac{1+ST_{1}^{1}}{1+ST_{2}^{1}} \quad (2)$$

$$\frac{X_{Modulation}}{\Delta_{\omega 2}} = \frac{SK_{\omega}^{2}}{1+ST_{W}^{2}} X \frac{1+ST_{1}^{2}}{1+ST_{2}^{2}} \quad (3)$$

Where is speed deviation of the generator rotor to the reference speed .The lead-lag controllers send the modulation control signal ,to the TCSC, as shown in Fig. 3, and the auxiliary control signal, to the SVC, as shown in Fig. 5. The lead-lag controllers help enhance the oscillation damping ability contributed by TCSC and SVC, thereby obtaining much higher levels of stable power transfer. To improve the control performance, instead of using fixed parameter sets and in the two lead-lag controllers, this paper proposes a fuzzy lead-lag control configuration in which all of the parameters in the two lead-lag controllers are adaptively adjusted through an FC.

B. Fuzzy Lead-Lag Controller

In the FC, there are three input variables, and which are speed deviations of the rotors in generatorsG2, G3, and G4, respectively. The outputs of the FC determine the values of the eight parameters in the two lead-lag controllers. The FC is composed of zero-order Takagi-Sugeno (TS)-type fuzzy IF-THEN rules with the following form:

Rule I: IF $\Delta_{\omega 2}$ (t) isA_1^i and $\Delta_{\omega 3}$ (t) isA_2^i AND $\Delta_{\omega 4}$ (t) isA_3^i, THEN $T_1^i\ isa_1^i$(t), $T_2^i\ isa_2^i$(t), $T_W^i\ isa_3^i$(t), $K_W^i\ isa_4^i$(t), $T_1^2\ isa_5^i$(t), $T_2^2\ isa_6^i$(t), $T_W^2\ isa_7^i$(t), $K_W^2\ isa_8^i$(t), i=1,…….R (4)

Where, is a crisp value, is the total number of rules, and each fuzzy set uses a Gaussian membership function, that is described by

$$\mu_j^i(\Delta_{\omega k}) = \exp\{(-\Delta_{\omega k} - m_j^i)2\backslash(b_j^i)2\} \quad (5)$$

Where and represent the center and width of the fuzzy set, respectively. The firing strength of the rule is computed by

$$\emptyset^i(x) = \mu_1^i(\Delta\omega_2).\mu_2^i(\Delta\omega_3).\mu_3^i(\Delta\omega_4). \quad (6)$$

The output of the FC described in (4) is denoted as, and is calculated by the following weighted average Defuzzification formula:

$$Y_m = (\sum_{l=1}^{R} \emptyset^l . a_m^i)\backslash\sum_{l=1}^{R} \emptyset^l \quad (7)$$

The rotor speed deviations of all generators are used as controller inputs in order to evaluate the damping effect and determine the parameters of lead-lag controllers simultaneously. A modern PS has hundreds of generators. In many cases, we can identify groups of generators that are closely coupled internally but relatively weakly coupled between groups. In addition, a reduced-order nonlinear system model can be derived from the original PS by aggregation techniques . Then, the proposed approach can be used.

IV. ADVANCED CONTINUOUS ANT COLONY OPTIMIZATION FOR FUZZY CONTROLLER OPTIMIZATION

A. Advanced Continuous Ant Colony Optimization (ACACO)

The proposed ACACO works with a constant colony size of solutions (ants) at each learning iteration .Initially, the solutions are randomly generated. Each solution vector represents all of the parameters in an FC, i.e., a solution vector represents an FC. The solutions are sorted according to their performances from the best to the worst, and therefore, solution has rank. Fig. 7 shows a graphical representation of the ACACO algorithm in terms of nodes and path segments. The node values, in the throw represent values of the optimized variables in solution vector. Each path segment is associated with a pheromone level. The performance of a better solution is assigned with a stronger pheromone level so that the node connected to it is selected with a higher probability. In other words, the order of the pheromone level amplitudes.

ACACO consists of two phases. In the first phase, ants start from the nest, move through nodes of variables and stop at the node of variable. The completion of the ant path constructs the temporary solution vector, denoted as where the values in the nodes visited constitute the temporary solution components .ACACO consists of two phases. In the first phase, ants start from the nest, move through nodes of variables, and stop at the node of variable. The completion of the ant path constructs the temporary solution vector, denoted as where the values in the nodes visited constitute the temporary solution components.

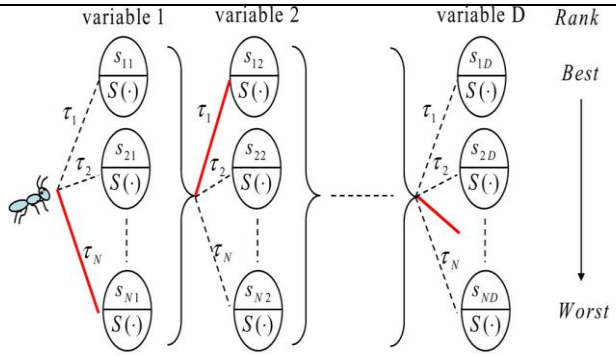

Fig. 7. Graphic representation of ACACO in terms of nodes and path segments, where an ant path is marked by a bold line.

Method generates new temporary solutions, where the ant simply selects all the path segments with pheromone level. In other words, the top ranked solution vectors stored in the colony serve as the temporary solutions, i.e., the tournament selection generates the other new temporary solutions. In the tournament selection, when an ant goes from variable to variable, three of the path segments are first selected randomly and uniformly, regardless of the pheromone levels. The pheromone levels on the three selected path segments are then compared, and the one with the highest level is finally selected. Fig. 7 shows a path selected by the tournament selection method. In RCACO, the number of temporary solutions generated from the two selections is the same at each iteration, i.e., As opposed to RCACO; ACACO uses a new distribution approach that dynamically adjusts the number of solutions between the elite and tournament selections to improve the search ability. The number in the elite selection varies with the iteration number, and is given by

$$\mathrm{L}\,(I_C) = Tx(\frac{I_C}{End-ite}) \quad (8)$$

Where "End ite" is the total number of iterations. Equation (8) shows that the number of solutions generated by the elite and tournament selections increase and decrease with iteration number, respectively. The second phase introduces new values to each node (solution component) via sampling of a Gaussian PDF and replacing the temporary solution component, with the new sampled value. The component serves as the mean of Similar to ACO in real space , the STD, of is computed as follows:

$$d_{ij} = \in . \sum_{t=1}^{N} s_{ij} - s_{ij} \,|\backslash (\text{N-1}) \quad (9)$$

Which is calculated according to the distance from the selected node value to the other node values for the same variable. The value of tends to decrease as learning converges. In , a constant value of is used in (9). This paper uses an adaptive described by

$$\in = f_{li} X \frac{I_c}{End\_ite} + f_{1f} \quad (10)$$

The value of increases from to as learning evolves to avoid premature convergence of the STD. Applying the Gaussian sampling operation to the temporary solution vector, , gives a new solution vector, denoted as in ACACO, where

$$s_i^{new} = [s_i^{new} \ldots\ldots, s_{id}^{new}] = [\mathrm{S}(g_{i1(s_{i1})}), \ldots\ldots, \mathrm{S}(g_{iD}(S_{iD}))], \mathrm{I}=1, \ldots..\mathrm{T}. \quad (11)$$

For each generation, a total of new solutions are generated, and these solutions are deposited with the original solutions. These solutions are sorted from the best to the worst according their performance (i.e., according their cost) values). ACACO works with a fixed solution size; therefore, only the best solutions are reserved, and the others are discarded.

B. FC Optimization through ACACO

In the ACACO-designed FC, the number of fuzzy rules is assigned in advance, and the number of fuzzy sets in each input variable is equal to the number of rules. All of the free parameters in the FC described in (4) are optimized. For the rule, there are two free parameters (and) for each of the three fuzzy sets in the antecedent part and eight free parameters in the consequent part, so the dimension of each solution vector is equal to Initially, a total of solution vectors, are generated. The performance of a solution vector is evaluated by a cost function that measures the control performance of the corresponding fuzzy lead-lag controller.

V. SIMULATIONS

The following simulations were conducted on an Intel Core 2 quad-core-processor 2.83 GHz, running the Windows 7 operating system. The sampling interval in all examples was set to 0.001 s.

A. Fuzzy Lead-Lag Control

Example 1 (Controller Design in Training Phase): To generate online training data for the performance Evaluation of a controller, this paper assumes that at 0.2 s, a sudden increment of 0.1 p.u. mechanical torque occurs simultaneously at all three generators, G2, G3, and G4, and that this increment disappears after 0.3 s. The control period is 0-9 s. Fig. 8 shows the dynamic response of the speed deviations and the angles of the rotors in generators G2, G3, and G4 without using the TCSC and SVC devices. The result shows that the system is nearly unstable without control. In applying ACACO to the evolutionary fuzzy lead-lag control problem, the rule number, was set at 5, the colony size was set at 20 and was set at 10. The number of iterations was set at 1000. That is, there were a total of performance evaluations per run. For statistical analysis, learning was repeated for 30 runs. For real-time operation, the FC should send control outputs to the PS within each sampling interval. In the simulations, it took only for the FC to send outputs for each new input data. Computations of the ACACO were performed only after the end of the whole control period. Therefore, the proposed approach is feasible for real-time training. The cost function, for performance evaluation was computed using the root-mean-squared deviations of generator rotor speeds, and angles, 3, and 4, over 9000 time steps. The cost function is described as shown

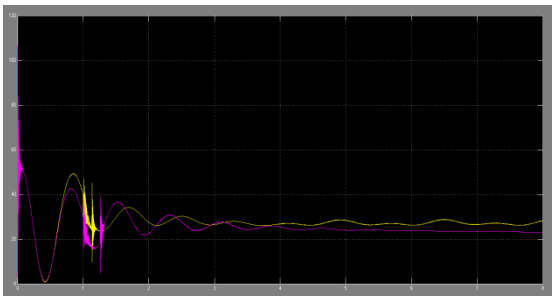

Fig. 8. Dynamic response of rotor speed deviations and angles in G2, G3, and G4 using fuzzy lead-lag controller, lead-lag controller and without control in Example 1, where a sudden increment of 0.1 p.u. mechanical torque occurs in G2, G3, and G4 at 0.2 s.

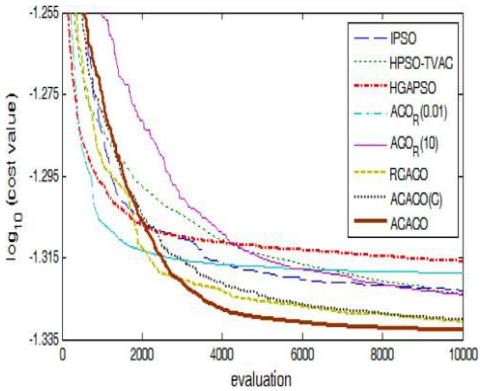

Fig. 9 Averaged best-so-far cost value at each evaluation for evolutionary fuzzy lead-lag control through ACACO and several modified continuous ACO and PSO algorithms.

In (12) at the bottom of the page. As shown in Fig. 8, the angle deviation is about one thousand times the scale of the speed deviation; therefore, weightings and were set to a large value of to improve system performance especially at low speed deviation values, such as. The speed deviation of generator G4 depends heavily on those of generators G2 and G3; therefore, the weighting was simply set to 1. The weightings , , and were all originally set to 1 and then reset to 100 for the last 3000 control time steps to improve the steady state response of the rotor angles. Fig. 9 shows the best-so-far average value of at each evaluation. Table

I shows the average (0.04650) and STD (0.00024) of the cost value, over the 30 runs. Fig. 8 shows the dynamic response of the best

TABLE I
LEARNING PERFORMANCE OF ACACO AND VARIOUS CONTINUOUS ACO ALGORITHMS FOR EVOLUTIONARY FUZZY LEAD-LAG CONTROL IN EXAMPLE1

Algorithms	ACO_R ($q = 0.01$) [22]	ACO_R ($q = 10$) [22]	RCACO [23]	ACACO(C)	ACACO
Average cost	0.04802	0.04743	0.04669	0.04675	0.04650
STD	0.001445	0.00067	0.00044	0.000460	0.00024
t-value	5.636	7.164	1.989	2.592	--

TABLE II
LEARNING PERFORMANCE OF ACACO AND VARIOUS MODIFIED PSO ALGORITHMS USING FUZZY LEAD-LAG CONTROLLER IN EXAMPLE 1

Algorithms	HPSO-TVAC [18]	HGAPSO [19]	IPSO [20]	ACACO
Average cost	0.047457	0.048321	0.047514	0.046504
STD	0.000780	0.000998	0.000559	0.000244
t-value	6.387	9.687	9.070	--

Fuzzy lead-lag controller under the training condition. The result shows that the fuzzy lead-lag controller successfully damps the system oscillations. For quantitative analysis of the control result, Table II shows the sum of absolute deviation (SAD) values for both and (3, and 4) over the control period 0-9 s. For the purpose of comparison, several modified continuous ACO and PSO algorithms were applied to the same evolutionary fuzzy lead-lag control problem. The modified continuous ACO algorithms used for comparison include with different coefficients and RCACO [23], and ACACO with a constant value of 0.85 in (9) [called ACACO(C)]. The modified PSO algorithms used for comparison include a hierarchical PSO with a time-varying acceleration coefficient (HPSO-TVAC) [18], a hybrid of the GA and PSO (HGAPSO) [19], and an improved PSO algorithm (IPSO) [20]. The population size and number of evaluations in these modified continuous ACO and PSO algorithms were set to be the same as those in the ACACO algorithm. Tables I and II show the performances of these continuous ACO and PSO algorithms, respectively. Fig. 9 shows the best-so-far average values of at each evaluation of these continuous ACO and PSO algorithms, respectively.
The result indicates that the average cost value is smaller for the ACACO algorithm than for the other algorithms used for comparison. For statistical analysis, this paper uses the -test to evaluate whether the difference between ACACO and the other algorithms is significant. Tables I and II show the -values. The null hypothesis is rejected at the 5% significance level for each pair of comparisons, which indicates the significant difference between the ACACO and the other algorithms.

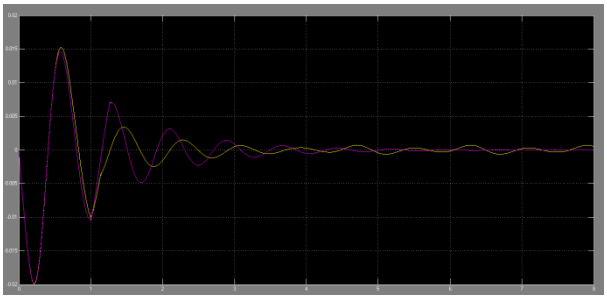

Fig.10. Dynamic response of rotor speed deviations and angles in G2, G3, and G4 using fuzzy lead-lag controller, lead-lag controller and without controlling Example 2.

TABLE III
PERFORMANCE OF FUZZY LEAD-LAG CONTROLLER AND LEAD-LAG CONTROLLER AT INCOMING SUDDEN INCREMENTS OF 0.01 P.U., 0.05P.U., AND 0.1 P.U. MECHANICAL TORQUE AT THE 2ND, 3RD, AND 4TH GENERATORS IN EXAMPLE 2

Σ	$\lvert\Delta\omega_2\rvert$	$\lvert\Delta\omega_3\rvert$	$\lvert\Delta\omega_4\rvert$	$\lvert\Delta\delta_2\rvert$	$\lvert\Delta\delta_3\rvert$	$\lvert\Delta\delta_4\rvert$
Lead-lag	0.001514	0.000398	0.002742	3.158593	0.749941	1.520297
Fuzzy lead-lag	0.001467	0.000315	0.001399	3.073404	0.653612	0.913832

He computational time for each run of the ACACO-based training approach took about 21 hours, which was about the same as those of the modified continuous ACO and PSO algorithms used for comparison. The reason is that the time was mainly spent on computations of the PS outputs at each of the evaluations. The computational time of each population based learning algorithm is almost negligible in comparison with the PS output computations.

Example 2 (Test Control With Different Amplitudes of Torque Increment): To test the performance of the fuzzy lead-lag controller designed in Example 1, the control of the three- machine PS with different torque perturbation amplitudes is studied in this example. It was supposed that there were incoming increments of mechanical torques in all of the three generators G2, G3, and G4with different amplitudes of 0.01p.u. 0.05p.u. and 0.1p.u. at 0.2 s, 6 s, and 15 s, respectively. Each increment disappeared after 0.1 s of its occurrence. Fig. 10 shows the dynamic response of the rotor speed deviations and the angles in generators G2, G3, and G4 without using the TCSC and SVC control. The results show that the system is undamped without control. Fig. 10 also shows the dynamic response obtained with the fuzzy lead-lag controller; the results show that the controller successfully damps the oscillations regardless of their amplitudes. For quantitative analysis, Table III shows the sum of absolute deviation (SAD) values of and 3, and 4) in the control period [0, 27] s. Example 3 (Test Control with Random Torque Perturbations at Different Generators): This example considers the test control problem where mechanical torque perturbations randomly

TABLE IV
PERFORMANCE OF FUZZY LEAD-LAG CONTROLLER AND LEAD-LAG CONTROLLER AT UNKNOWN PERTURBATION AT THE 2ND, 3RD, AND 4TH TRANSMISSION LINES IN EXAMPLE 3

Σ	$\lvert\Delta\omega_2\rvert$	$\lvert\Delta\omega_3\rvert$	$\lvert\Delta\omega_4\rvert$	$\lvert\Delta\delta_2\rvert$	$\lvert\Delta\delta_3\rvert$	$\lvert\Delta\delta_4\rvert$
Lead-lag	0.000439	0.000134	0.000329	0.874215	0.215034	0.215149
Fuzzy lead-lag	0.000429	0.000078	0.000075	0.830994	0.136603	0.061266

Occur in one of the three generators, G2, G3, and G4. Three torque perturbations were randomly generated in the time interval [0, 5] s with magnitudes that were randomly and uniformly generated from the interval [0, 0.1] p.u. The duration of each perturbation lasted 0.1 s. The first increment of 0.085 p.u. mechanical torque occurred in G2 at 2.23 s, where it can be observed that the other two generators were also indirectly affected. At 3.33 s and 3.72 s, there were sudden increments of0.01 p.u. and 0.045 p.u. mechanical torques in G4 and G3, respectively. Fig. 11 shows that the dynamic response is unstable without using the TCSC and SVC control. Fig. 11 also shows the dynamic response when using the fuzzy lead-lag controller. The results show that the controller successfully damps the oscillations regardless of the generators at which the perturbation occurs. Table IV shows the SAD values of and in the control period [0, 12] s.

Example 4 (Test Control with Faulted Lines): This example considers the contingency that a three-phase fault occurs on the transmission line between buses 1 and 2 in Fig. 1. It is assumed that at 0.2 s fault occurs on the line and recloses at 0.3 s in the time interval [0, 7] s. Fig. 12 shows the dynamic response using the fuzzy control. The results show that controller successfully damps the oscillations. Table V shows the SAD vales of and (, 3, and 4) in the control period [0, 7] s.

B. Comparisons with Lead-Lag Controllers

This subsection replaces the fuzzy lead-lag controller in Examples 1 to 4 with the lead-lag controllers in (2) and (3) for

TABLE V
PERFORMANCEOFFUZZYLEADLAGCONTROLLER AND LEAD-LAG CONTROLLER WHEN A FAULT OCCURS ON THE TRANSMISSION LINE BETWEEN BUSES 1 AND 2 IN EXAMPLE 4

Σ	$\lvert\Delta\omega_2\rvert$	$\lvert\Delta\omega_3\rvert$	$\lvert\Delta\omega_4\rvert$	$\lvert\Delta\delta_2\rvert$	$\lvert\Delta\delta_3\rvert$	$\lvert\Delta\delta_4\rvert$
Lead-lag	0.000196	0.000087	0.000871	0.467342	0.193137	0.465241
Fuzzy lead-lag	0.000156	0.000045	0.000578	0.366689	0.121561	0.304135

Comparative analysis. The parameter sets of the two lead-lag controllers were optimized using ACACO with the cost function in (12) and the training condition used in the fuzzy lead-lag controller in Example 1. The average and STD of the cost value, , over 30 runs were 0.04813 and 0.00015, respectively. In comparison with the fuzzy lead-lag controller result shown in Table I, the -value was 31.151 and the null hypothesis was rejected at the 1%significance level. In other words, the training performance of the fuzzy lead-lag controller is significantly better than the lead-lag controller. Figs. 8 and 10–12 show the dynamic responses of the PS using the best-learned lead-lag controller in Examples 1 to 4. The lead-lag controller also successfully damps the oscillations in all examples. However, the results show that the fuzzy lead-lag controller damps the oscillations much more efficiently than the lead-lag controller. For quantitative analysis, Tables III–V shows the SAD values of and in Examples 2, 3, and 4, respectively, when using the lead-lag controller. The results show that all of the values in the different examples are smaller when using the fuzzy lead-lag controller versus the lead-lag controller, which verifies the advantage of using the proposed fuzzy lead-lag controller .Finally, it should be mentioned that this paper does not consider the important issue of communication time delays on a wide area control system in practice . In our proposed approach, it is possible to take the time delay effects into account by introducing a suitable amount of additional phase lag transfer function into the lead-lag controller for a fixed time-delay communication link. And then the CCACO-designed approach is employed to find the optimal fuzzy lead-lag controller for the time-delay system. The time delay will become a significant limitation in the design and operation when it is time variant. To address this problem, the incorporation of measurement/control signal predictors, such as the adaptive neural network predictor [28], into the proposed control approach will be studied in the future.

VI. CONCLUSION

This paper proposes the combination of two FACTS devices, an SVC and a TCSC, for the stabilization of a multi-machine PS. Simulation results in various conditions with different torque perturbations verify the Oscillation damping ability of the evolutionary fuzzy lead-lead control approach. In addition, comparison with the traditional lead-lag control approach shows the advantage of introducing the FC to adaptively determine the parameters in lead-lag controllers according to system status. The simulation results show that automatic optimization of the FC through the ACACO algorithm not only simplifies the design effort but also improves the system dynamic response. Comparisons with various modified continuous ACO and PSO algorithms show the advantage of using the ACACO algorithm in the PS stabilization problem.

REFERENCES

[1]. P. Kundur, J. Paserba, V. Ajjarapu, G. Andersson, A. Bose, C.Canizares, N. Hatziargyiou, D. Hill, A. Stankovic, C. Taylor, T.Cutsem, and V. Vittal, "Definition and classification of power system stability," *IEEE Trans. Power Syst.*, vol. 19, no. 2, pp. 1387–1401,May 2004.

[2]. J. J. Sanchez-Gasca, "Coordinated control of two FACTS devices fordamping interarea oscillations," *IEEE Trans. Power Syst.*, vol. 13, no.2, pp. 428–434, May 1997.

[3]. R. Mohan. Mathur and R. K. Varma, *Thyristor-Based FACTS ControllerFor Electrical Transmission System*. Piscataway, NJ: IEEE Press/Wiley Interscience, 2002.

[4]. K. Clark, B. Fradanesh, and R. Adapa, "Thyristor-controlled seriescompensation application study—Control interaction considerations,"*IEEE Trans. Power Del.*, vol. 10, no. 2, pp. 1031–1037, Apr. 1995.

[5]. D. P. He, C. Y. Chung, and Y. Xue, "An eigenstructure-based performanceindex and its application to control design for damping interarea oscillations in power systems," *IEEE Trans. Power Syst.*, vol. 26,no. 4, pp. 2371–2380, Nov. 2011.

[6]. Y. C. Chang, R. F. Chang, T. Y. Hsiao, and C. N. Lu, "Transmissionsystem locability enhancement study by ordinal optimization method,"*IEEE Trans. Power Syst.*, vol. 26, no. 1, pp. 451–459, Feb. 2011.

[7]. X. Tan, N. Zhang, L. Tong, and Z. Wang, "Fuzzy control of thyristorcontrolleredseries compensator in power system transients," *FuzzySets Syst.*, vol. 110, pp. 429–436, 2000.

[8]. X. Lei, E. N. Lerch, and D. Povh, "Optimization and coordination ofdamping controls for improving system dynamic performance," *IEEETrans. Power Syst.*, vol. 16, no. 3, pp. 473–480, Aug. 2001.

[9]. N. Mithulananthan, C. A. Canizares, J. Reeve, and G. J. Rogers,"Comparison of PSS, SVC, and STATCOM controllers for dampingpower system oscillations," *IEEE Trans. Power Syst.*, vol. 18, no. 2, pp. 786–792, May 2003.

[10]. M. E. Aboul-Ela, A. A. Sallam, J. D. McCalley, and A. A. Fouad,"Damping controller design for power system oscillations using globalsignals," *IEEE Trans. Power Syst.*, vol. 11, no. 2, pp. 767–773, May1996.

[11]. U. P. Mhaskar and A. M. Kulkarni, "Power oscillation damping usingFACTS devices: Model controllabiliby, observability in local signals, and location of transfer function zeros," *IEEE Trans. Power Syst.*, vol. [11] U. P. Mhaskar and A. M. Kulkarni, "Power oscillation damping using FACTS devices: Model controllabiliby, observability in local signals,and location of transfer function zeros," *IEEE Trans. Power Syst.*, vol.21, no. 1, pp. 285–294, Feb. 2006.

[12]. A. M. Simões, D. C. Savelli, P. C. Pellanda, N. Martins, and P. Apkarian,"Robust design of a TCSC oscillation damping controller in a week 200-kv interconnection considering multiple power flow scenariosand external disturbances," *IEEE Trans. Power Syst.*, vol. 24,no. 1, pp. 226–236, Feb. 2009.

[13]. P. K. Dash, S. Morris, and S. Mishra, "Design of a nonlinear variablegainfuzzy controller for FACTS devices," *IEEE Trans. Control Syst. Technol.*, vol. 12, no. 3, pp. 428–438, May 2004.

[14]. C. F. Lu and C. F. Juang, "Evolutionary fuzzy control of flexible ACtransmission system," *Proc. Inst. Elect. Eng., Gener.,Transm. Distrib* vol. 152, no. 4, pp. 441–448, Jul. 2005.

[15]. C. F. Juang, "Temporal problems solved by dynamic fuzzy networkbased on genetic algorithm with variable-lengthchromosomes